Available online at www.sciencedirect.com
SCIENCE DIRECT®
C. R. Chimie 8 (2005) 1298–1307
COMPTES RENDUS CHIMIE
http://france.elsevier.com/direct/CRAS2C/

Full paper / mémoire

Synthesis of star-shaped metallo-polymeric chromophores by atom transfer radical polymerization

Lydie Viau [a], Michael Even [b], Olivier Maury [a], David M. Haddleton [b], Hubert Le Bozec [a,*]

[a] *Institut de chimie, UMR 6509 CNRS, université Rennes-1, campus de Baulieu, 35042 Rennes cedex, France*
[b] *Department of Chemistry, University of Warwick, Coventry CV4 7AL, UK*

Received 13 July 2004; accepted after revision 16 November 2004

Available online 19 March 2005

Dedicated to Professor David Carillo on the occasion of his 65th birthday

Abstract

The synthesis of bromoester-functionalized dialkylaminostyryl-2,2′-bipyridyl ligands and of the corresponding tris[dialkylaminostyryl-2,2′-bipyridine] metal(II) complexes are reported (M = Fe, Ru, Zn). These complexes are used as multifunctional metallo-initiators for the atom transfer radical polymerization (ATRP) of methyl methacrylate. The resulting new star-shaped polymers combine the optical (UV–visible and luminescence) properties of the monomers with good processability, which allow to build high optical quality thin films by the spin-coating technique. ***To cite this article: L. Viau et al., C. R. Chimie 8 (2005)***.

Résumé

La synthèse de deux (dialkylaminostyryl)-2,2′-bipyridines fonctionnalisées par des groupements bromoesters est décrite. Ces ligands permettent d'accéder à des complexes de type tris(bipyridyl) métal(II) (M = Fe, Ru, Zn), qui sont des initiateurs pour la polymérisation radicalaire par transfert d'atome du méthacrylate de méthyle. Les polymères en étoile résultants ont été caractérisés par les spectroscopies UV–visible et d'émission. Ils conservent les propriétés optiques des complexes monomères parents et leurs excellentes solubilités ont permis d'élaborer des films de bonne qualité optique par la technique de *spin-coating*. ***Pour citer cet article : L. Viau et al., C. R. Chimie 8 (2005)***.

Keywords: ATRP; Star polymers; Chromophores; Coordination chemistry; Bipyridine ligands

Mots clés : ATRP ; Polymères en étoile ; Chromophores ; Chimie de coordination ; Ligands bipyridines

* Corresponding author.
E-mail address: lebozec@univ-rennes1.fr (H. Le Bozec).

1631-0748/$ - see front matter © 2005 Académie des sciences. Published by Elsevier SAS. All rights reserved.
doi:10.1016/j.crci.2004.11.034

1. Introduction

A new approach to well-defined macromolecules with architectural control involves the metal-mediated living radical polymerization (ATRP). Since the pioneering work of Matyjaszewski [1] and Sawamoto [2], this technique has been widely used to prepare polymers, co-polymers as well as star dendritic-polymers [3] from a variety of monomers and metal catalysts [4]. This strategy has also been recently used to the synthesis of star-shaped polymers with metal tris(bipyridyl) reagents as initiators [5].

Over the past decade, we have been concerned with the NLO properties of 4,4′-disubstituted-2,2′-bipyridine metal complexes [6]. We have demonstrated that these ligands are excellent building blocks for the construction of octupolar either octahedral or pseudo-tetrahedral complexes, and offer many possibilities for the design of noncentrosymmetric NLO-phores [7]. An important challenge is now the translation of microscopic to macroscopic noncentrosymmetric orientation of octupolar chromophores by the so called 'all optical poling' [8]. Basically, this method requires the preparation of polymer films containing NLO chromophores featuring photoisomerizable moieties. With the reasonable expectation that the ATRP strategy could offer a convenient entry to a variety of octupolar polymeric NLO-phores, we first sought to design a 2-bromoisobutyroyl-functionalized dialkylaminostyryl bipyridine as a model ligand. Herein we report the synthesis of this new chromophore and of the corresponding zinc, ruthenium and iron complexes. We show that these complexes are efficient metallo-initiators for the living radical polymerization of MMA and give rise to new star-shaped metallopolymers, which combine the optical properties of the monomers with good processability [9].

2. Results and discussion

2.1. Ligand synthesis

As haloesters have been successfully employed to initiate ATRP [1], we introduced a bromoester group at the amino electrodonating site of dialkylaminostyryl-2,2′-bipyridyl ligands. Bipyridines **b** and **b′** were obtained in good yields upon esterification of the hydroxy-functionalized 4,4′-dialkylaminostyryl-2,2′-bipyridines [10] **a** and **a′** with 2-bromoisobutyroyl bromide in the presence of pyridine at room temperature (Fig. 1).

These two new ligands were fully characterized by NMR, UV–visible, emission spectroscopy and mass spectrometry, and gave satisfactorily microanalyses. The optical and thermal properties of **b** and **b′** as well as those of the parent ligands 4,4′-diethylaminostyryl-2,2′-bipyridine **DEASbpy** and 4,4′-dibutylaminostyryl-2,2′-bipyridine **DBASbpy** are summarized in Table 1.

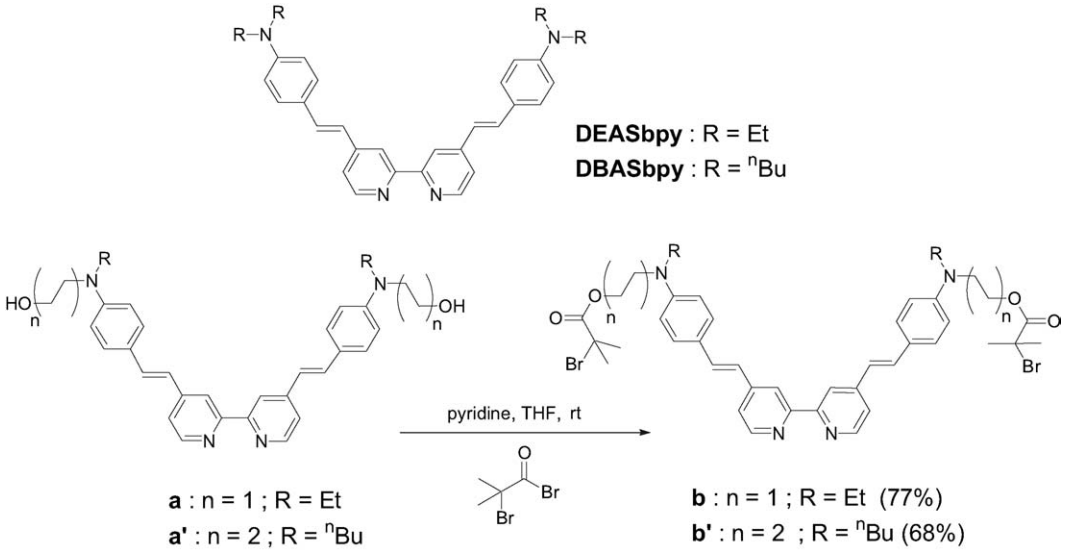

Fig. 1. Synthesis of bipyridyl ligands.

Table 1
Optical and thermal properties of ligands, complexes and polymers.

Compound	λ_{ILCT} [a] (ε); λ_{MLCT} (ε) nm ($l\ mol^{-1}\ cm^{-1}$)	λ_{em} [a] (nm)	T_{d10} [b] (°C)	T_g [c] (°C)
DEASbpy	397 (57, 000)	495	330	
DBASbpy	400 (65, 000)	497	381	
b	385 (55, 000)	486	210	
b′	391 (40, 200)	495	210	
1b (Fe)	456 (138, 000); 589 (56, 000)	621	210	
2b (Ru)	438 (91, 000); 501 (85, 000)	713	190	
3b (Zn)	448 (146, 000)	620	235	
1c (Fe) solution	452; 577	622	285	124
1c (Fe) film	443; 582	–[d]		
2c (Ru) solution	440; 503	711	310	126
2c (Ru) film	430; 500	–[d]		
3c (Zn) solution	442	608	295	124
3c (Zn) film	450	–[d]		

[a] Measured in dichlomethane solution ($c = 1 \times 10^{-5}$ mol l^{-1}).
[b] TGA, 10 °C/min.
[c] DSC, 10 °C/min.
[d] Not measured.

They show a typical intense, structureless and large intraligand charge-transfer band at 385–391 nm, which is blue-shifted by ca. 10 nm as compared to the λ_{max} of **DEASbpy** and **DBASbpy**. This hypsochromic shift can be easily explained by the electron withdrawing effect of the bromoester groups. Likewise, **b** and **b′** display a slightly blue-shifted emission band at 486 and 495 nm, respectively. A more dramatic change was observed by comparing the thermal properties (Td_{10} determined by TGA) of **b**/**b′** vs. **DEASbpy**/**DBASbpy** (Table 1). Whereas the parent ligands are stable at more than 300 °C, the thermal stabilities of **b** and **b′** decrease considerably ($T_{d_{10}} = 210$ °C). To get more insight into this spectacular Td drop down, we heated **b** in refluxing DMF, which is the common solvent used for complexation to Ruthenium(II). After synthetic workup a new bipyridyl ligand **c**, corresponding to the loss of two HBr, was characterized by NMR and mass spectrometry (Fig. 2). Thus, the rather weak thermal stability of **b** (and **b′**) could be due to this easy dehydrohalogenation process.

2.2. Metalloinitiator synthesis

Two strategies were used for the synthesis of Ruthenium(II), Iron(II) and Zinc(II) complexes **1b**–**3b**, depending on the nature of the metal salt. Sonochemically assisted room temperature reaction of **b** (3 equiv.) with iron sulfate in acetone/water, followed by an anionic exchange with PF_6^-, yielded **1b** as a greenish black microcrystalline powder in 75% yield (Fig. 3). However, this route could not be used to prepare the corresponding ruthenium complex **2b**, due to the dehydrobromination process in refluxing DMF.

Thus, **2b** was obtained by a second route (Fig. 4) in a two-step synthesis: (*i*) the deep red complex **2a** bearing six hydroxy groups was first prepared in 83% yield upon treatment of $RuCl_2(dmso)_4$ with 3 equiv. of **a**, followed by an anionic metathesis; (*ii*) treatment at room temperature of **2a** with an excess of 2-bromoisobutyroyl bromide in THF, in the presence of pyridine, yielded **2b** in 70%. The same methodology was employed to prepare the zinc complex **3b** which was isolated in 60% yield as an orange-red powder. Complexes **1b**–**3b** were characterized by ^1H and ^{13}C NMR spectroscopy and microanalysis (see Section 4) as well as by UV–visible and emission spectroscopy. The UV–visible spectra are very similar to those of the parent complexes (Table 1). The iron compound **1b** displays two well separated charge-transfer bands at 456 and 589 nm corresponding to the ILCT and MLCT transitions, respectively. As expected, the ruthenium complex **2b** exhibits an overlap of these two transitions at 438 and 501 nm (Fig. 8), whereas the absorption spectrum of zinc com-

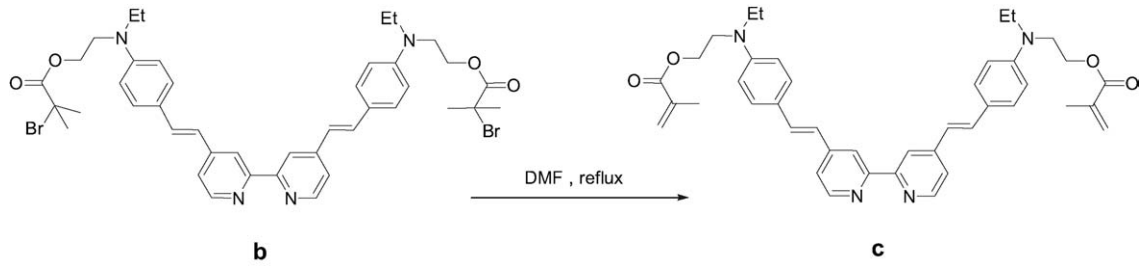

Fig. 2. Dehydrobromination process of ligand **b**.

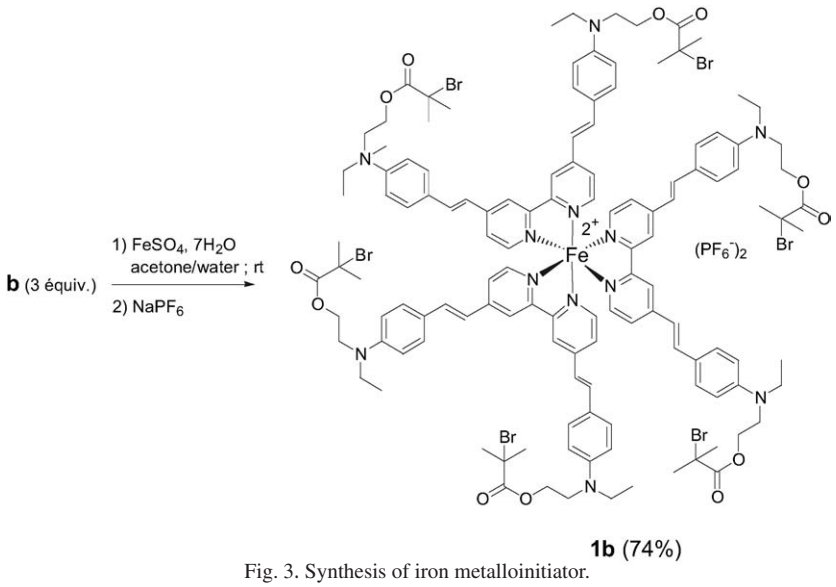

Fig. 3. Synthesis of iron metalloinitiator.

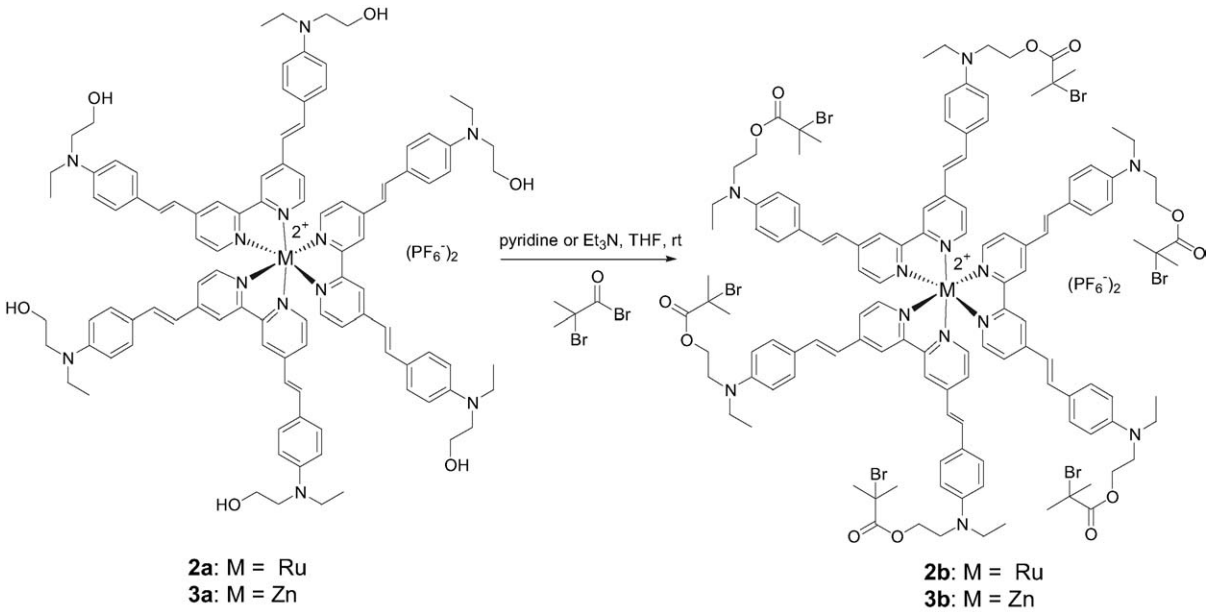

Fig. 4. Synthesis of ruthenium and zinc metalloinitiators.

plex **3b** shows only one ILCT band at 448 nm. Photoluminescence similar to that of the parent tris-bipyridyl metal complexes is observed for **1**–**3b** in diluted dichloromethane solution (Table 1). Iron(II) and Zinc(II) complexes **1b** and **3b** exhibit a broad, intense structureless emission band at 620 nm assigned to ligand-centered emission with very large Stokes shifts (5827 and 6192 cm^{-1}, respectively). By contrast, upon excitation at the MLCT or the ILCT wavelength, ruthenium complex **2b** features a red-shifted photoluminescence at 713 nm (Table 1). The excitation spectrum overlays the absorption spectrum with two maxima corresponding to the ILCT and MLCT transitions, indicating that the observed emission arises from MLCT triplet states [11].

2.3. Star-shaped polymers

ATRP of MMA was carried out in 1,2-dichlorobenzene at 90 °C using a 2:1:1 ratio of *N*-propyl-2-pyridylmethanimine [12]: CuBr: **1b**, **2b** or **3b** as initiator (In) and [MMA]: [In] = 260: 1. The resulting polymers **1c**–**3c** (Fig. 5) were obtained as green (Fe), brown (Ru) and orange (Zn) flocculent powders, respectively, after purification by column chromatography on alumina (eluent: CH_2Cl_2) and precipitation in CH_2Cl_2/pentane. Molecular weight characterizations were determined in toluene using GPC equipped with a differential refractive index (DRI) detector. The monomer conversion was analyzed every 30 min and representative data for different reaction times are summarized in Table 2. The rate of polymerization strongly depends on the nature of the metalloinitiator: whereas a conversion of 94% was achieved after 4 h with **3b** (Zn), only 50% conversion was reached when **2b** (Ru) was used. Kinetic plots of the three polymerizations show a first-order behavior consistent with a living system (Fig. 6). We also observed an induction period of approximately 25 min for the iron and ruthenium complexes. This induction period is frequently observed and is not fully understood. It could be due to the presence of residual oxygen [13]. It is noteworthy that the molecular weight distribution remains quite high and increased throughout the polymerization, especially in the case of **3c** where loss of control of the PDI was observed, reaching 3.47 at 94% conversion. At first glance, this could be due to termination reactions, but no higher molecular weight could be observed by GPC. As these results (low molecular weights and high PDI) seemed to be surprising, we carried out the molecular weight analysis of polymer **3c** by a GPC equipped with DRI and low angle laser light scattering (LALLS) detectors. The data are summarized in Table 3 and Fig. 7 shows that M_n increases linearly with conversion while the PDI remains consistently low. As can be seen in Table 3, the experimental and theoretical values of M_n correspond well. These results are thus consistent with a living atom transfer radical polymerization.

The UV–visible and emission spectra of these new polymers display absorption and emission bands very similar to those of the corresponding metallo-initiators **1b**, **2b** and **2b**, clearly indicating that the metallo-chromophoric structure is conserved upon polymerization (see Table 1 and Fig. 8 for the ruthenium complex). Thermal characterizations were performed by TGA and DSC (Table 1). They exhibit good thermal stability, with 10% weight losses ($T_{d_{10}}$) occurring at ca. 290 °C. It is noteworthy that the thermal stabilities of **1c**–**3c** are increased as compared to those of the corresponding metallo-initiators **1b**–**3b**, which undergo dehydrohalogenation reactions. The glass-transition temperature (T_g) is found at ca. 125 °C, a temperature

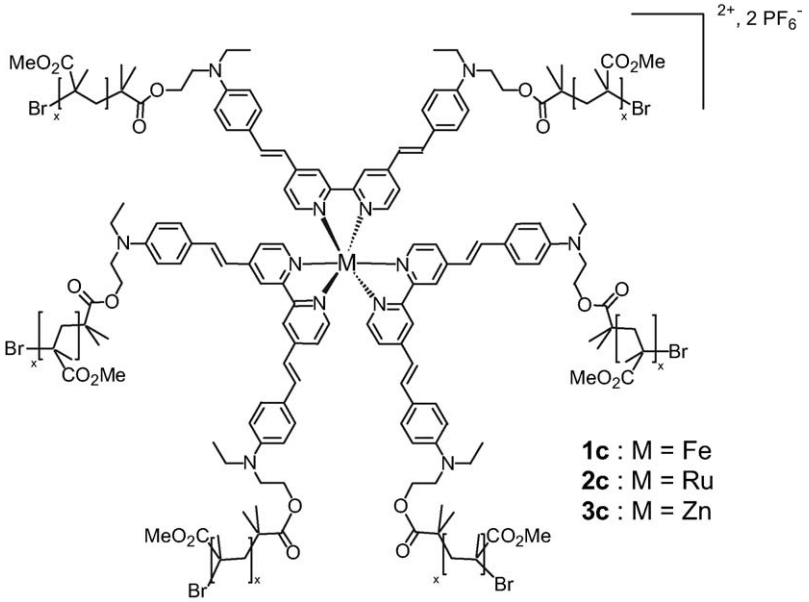

Fig. 5. Chemical structures of star-shaped polymers.

Table 2
Polymerization of MMA with initiators **1b**, **2b** and **3b**

Initiator	Time (min)	Conversion (%)[a]	M_n[b]	M_w[b]	PDI	Calc. M_n
1b (Fe)	30	7	4850	6000	1.24	13, 900
1b (Fe)	60	14	9010	12, 200	1.35	25, 400
1b (Fe)	90	29	10, 400	15, 100	1.45	49, 800
1b (Fe)	120	50	22, 000	29, 600	1.34	82, 500
1b (Fe)	180	73	32, 400	43, 300	1.33	119, 000
1b (Fe)	250	81	31, 740	53, 000	1.67	132, 500
2b (Ru)	30	0	0	0		3000
2b (Ru)	60	15	1000	1200	1.24	26,500
2b (Ru)	90	18	2100	2700	1.27	31, 500
2b (Ru)	120	28	3300	4300	1.32	49, 000
2b (Ru)	180	44	4200	5600	1.34	74, 500
2b (Ru)	240	50	5500	7400	1.36	83, 700
3b (Zn)	30	25	16, 200	20, 100	1.23	39, 900
3b (Zn)	60	47	24, 800	36, 300	1.46	72, 600
3b (Zn)	90	65	27, 400	53, 000	1.93	100, 400
3b (Zn)	120	78	28, 700	63, 300	2.20	119, 000
3b (Zn)	180	89	24, 500	76, 800	3.13	137, 000
3b (Zn)	240	94	24, 500	84, 900	3.47	143, 000

[a] Determined by gravimetry.
[b] Determined by GPC with DRI detector (solvent: THF).

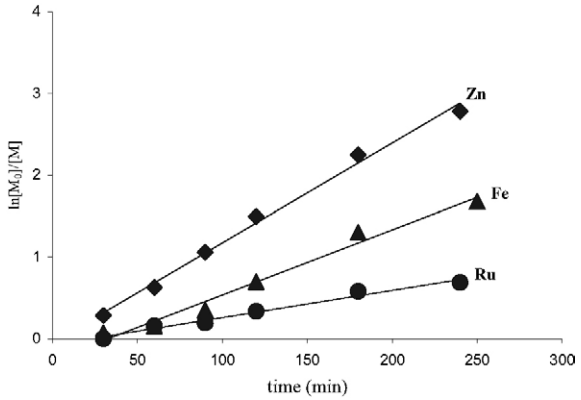

Fig. 6. Kinetics of the polymerization reactions using initiators **1b** (▲), **2b** (●) and **3b** (◆).

that is comparable to values reported in the literature for linear [13] and star-shaped [4] PMMA prepared by ATRP.

Finally, thin films were easily obtained by spin-coating a trichloro-1,2-ethane solution of **1c**–**3c** onto glass slides. Scanning electron microscopy (SEM) reveals the formation of very uniform films without any chromophore aggregation, and a thickness varying approximately between 1 and 2 μm (see Fig. 9 for the ruthenium polymer film). Solid state UV–visible spectroscopy (Table 1 and Fig. 8 for the ruthenium polymer

Table 3
Polymerization of MMA with initiator **3b**

Time (min)	Conversion (%)[a]	M_n[b]	M_w[b]	PDI	Calc. M_n
30	25	16, 900	20, 400	1.20	39, 900
60	47	58, 500	59, 700	1.02	72, 600
90	65	86, 700	87, 800	1.01	100, 400
120	78	117, 500	119, 300	1.01	119, 000
180	89	141, 400	145, 000	1.02	137, 000
240	94	173, 900	175, 500	1.01	143, 000

[a] Determined by gravimetry.
[b] Determined by GPC using DRI and LALLS detectors (solvent: THF).

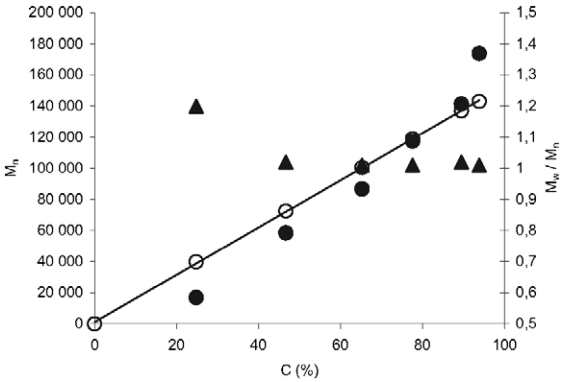

Fig. 7. M_n (●), calc. M_n (○) and PDI (▲) vs. conversion of the polymerization reaction using initiator **3b** (Zn).

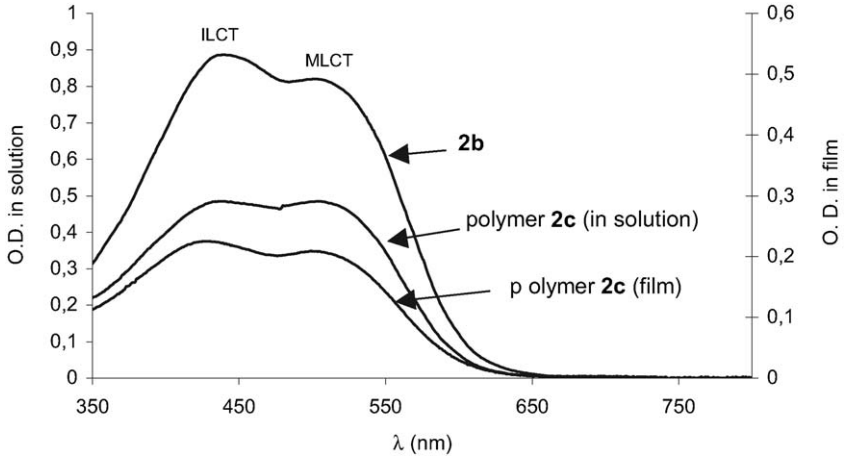

Fig. 8. UV–visible spectra of initiator **2b** (CH_2Cl_2) and polymer **2c** (CH_2Cl_2 and film).

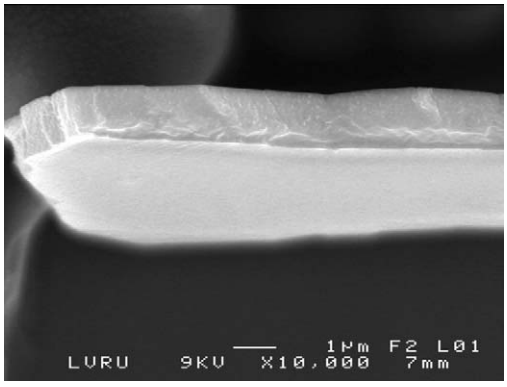

Fig. 9. SEM image of polymer **2c** (Ru).

film) unambiguously confirmed that the metallic tris-(bipyridyl) chromophores remain intact within the film.

3. Conclusion

In summary, this study shows that ATRP of methyl methacrylate with functionalized metallo-initiators is a very efficient and general method to prepare star-shaped polymers featuring octupolar NLO chromophores. Futhermore, these polymers are highly soluble in chlorinated solvents, which allow to build high optical quality thin films. Moreover, according to the UV–visible data, the structure of the incorporated complexes is not altered during the polymerization and the process. As a challenging work, we are now focusing on the bulk NLO-studies, particularly on the elaboration of films containing photoisomerizable octupolar metallo-chromophores [14] for 'all-optical' poling purpose in order to transfer the second-harmonic generation (SHG) from molecular to macroscopic level.

4. Experimental section

4.1. General data

All experiments were carried out using Schlenk vessel under inert atmosphere. NMR spectra were recorded at room temperature on a BRUKER DPX 200 spectrometer. UV–visible spectra were performed on a KONTRON UVIKON 941 in diluted dichloromethane solution (ca. 10^{-5} mol l^{-1}). Solid-state UV–visible spectra were obtained as thin films (prepared by spin coating) on a Perkin Elmer Lambda 2000 spectrophotometer. Routine fluorescence measurements were done using a Photon Technology International spectrophotometer. Infrared spectra were recorded in KBr pellets with a Nicolet FTIR spectrometer. Molar mass distributions were measured using size exclusion chromatography (SEC) at ambient temperature, on a system equipped with a guard column one 3-μm mixed E column (Polymer Laboratories) with DRI detection using tetrahydrofuran as eluent, at a flow rate of 1 ml min^{-1}. Poly(MMA) standards in the range (6 × 104–200 g mol^{-1}) were used for specific calibration. A $dn/dc = 0.086$ for poly(MMA) was used to calculate LALLS molecular weights. High resolution mass spectrometry (HRMS) and elemental analysis were carried out in the 'Centre de mesures physiques de l'Ouest' in

Rennes. SEM pictures were performed in the 'Centre de microscopie électronique à balayage et microanalyse' in Rennes on a Jeol Scanning Electron Microscope JSM-6301F. Tetrahydrofuran was dried and distilled before used over Na/benzophenone, pyridine was just distilled before used. bipyridines **a** and **a′**, and complex **3a** were synthesized using an already described procedure [10]. *N*-Propyl-2-pyridylmethanimine was synthesized as previously reported [12] and stored under anhydrous conditions prior to use. Copper(I) bromide (Aldrich, 98%) was purified according to the method of Keller and Wycoff [15]. MMA was obtained from Aldrich and filtered before utilization through a basic alumina column to remove the radical inhibitor. 2-Bromoisobutyroyl bromide, 1,2-dichlorobenzene, zinc acetate dihydrate and iron sulfate heptahydrate were obtained from Acros and used as received.

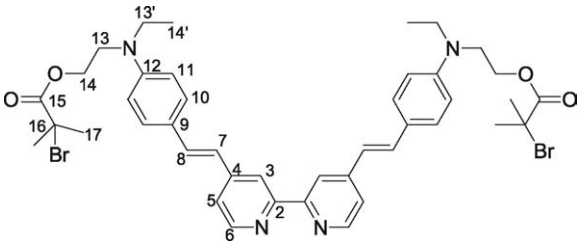

*4.1.1. 4,4′-Bis{N-ethyl-N-[2-(2-bromoisobutyroylester)ethyl]aminostyryl}-[2,2′]-bipyridine (**b**)*

A solution of 2-bromoisobutyroylbromide (1.27 ml, 10 mmol) in THF (15 ml) was added dropwise to a solution of the hydroxy functionalized ligand **a** (1.83 g, 3.4 mmol) and pyridine (0.7 ml, 8.5 mmol) in THF (50 ml). After being stirred overnight at room temperature, the reaction mixture was poured into aqueous HCl (40 ml, 4 N). The organic layer was separated and the aqueous layer was extracted with CH_2Cl_2 (3 × 100 ml). The combined organic layers were washed with an aqueous solution of NaOH (3 × 50 ml, 1 M), dried over $MgSO_4$, filtered and the solvents were removed under vacuum. The product was purified by precipitation from ether/pentane (1:2) to afford a brown powder (2 g, 70%).

^{1}H NMR ($CDCl_3$) δ ppm: 8.69 (d, J = 5.1 Hz, 2H, H_6), 8.56 (s, 2H, H_3), 7.6–7.3 (m, 8H, H_8, H_5, H_{10}), 6.89 (d, J = 16.2 Hz, 2H, H_7), 6.79 (d, J = 8.9 Hz, 4H, H_{11}), 4.42 (t, J = 6.1 Hz, 4H, H_{14}), 3.75 (t, J = 6.1 Hz, 4H, H_{13}), 3.49 (q, J = 7 Hz 4H, $H_{13'}$), 1.98 (s, 12H, H_{15}), 1.22 (t, J = 7 Hz, 6H, $H_{14'}$). ^{13}C NMR ($CDCl_3$) δ ppm: 172.2 (C_{15}), 156.5 (C_2), 149.5 (C_6), 148.3 (C_{12}), 147.3 (C_4), 134.0 (C_8), 129.1 (C_{10}), 124.9 (C_9), 121.8 (C_7), 121.0 (C_5), 118.3 (C_3), 112.3 (C_{11}), 63.7 (C_{14}), 55.9 (C_{16}), 48.7 (C_{13}), 45.7 ($C_{13'}$), 31.2 (C_{17}), 12.7 ($C_{14'}$). UV–visible (CH_2Cl_2): λ_{max} = 385 nm, ϵ_{max} = 55,000 l mol^{-1} cm^{-1}. Emission (CH_2Cl_2): λ_{em} = 486 nm. Anal. Calc. (found) for $C_{42}H_{48}N_4O_4Br_2{\cdot}1.5CH_2Cl_2$: C, 54.36 (54.70); H, 5.45 (5.50); N, 5.84 (6.27). HRMS (FAB) calc. for $C_{42}H_{49}N_4O_4Br_2$ $[M + H]^+$: 833.2105, found: 833.2057 uma.

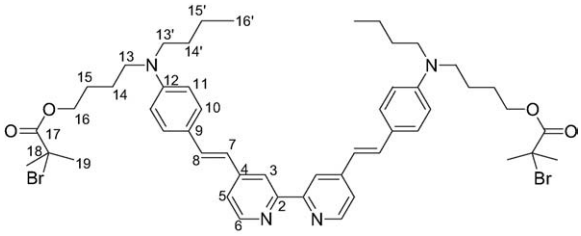

*4.1.2. 4,4′-Bis{N-butyl-N-[2-(2-bromoisobutyroylester)butyl]aminostyryl}-[2,2′]-bipyridine (**b′**)*

A solution of 2-bromoisobutyroylbromide (0.17 ml, 1.4 mmol) in THF (15 ml) was added dropwise to a solution of the hydroxy functionalized ligand **a′** (0.3 g, 0.46 mmol) and pyridine (0.1 ml, 1.2 mmol) in THF (10 ml). After being stirred overnight at room temperature, the reaction mixture was poured into aqueous HCl (20 ml, 4 N). The organic layer was separated and the aqueous layer was extracted with CH_2Cl_2 (3 × 50 ml). The combined organic layers were washed with an aqueous solution of NaOH (3 × 50 ml, 1 M), dried over $MgSO_4$, filtered and the solvents were removed under vacuum. The product was purified by precipitation from ether to afford a brown powder (0.28 g, 68%).

^{1}H NMR ($CDCl_3$) δ ppm: 8.65 (d, J = 5.3 Hz, 2H, H_6); 8.59 (s, 2H, H_3); 7.6–7.4 (m, 8H, H_8, H_5, H_{10}); 6.98 (d, J = 16.4 Hz, 2H, H_7); 6.73 (d, J = 8.8 Hz, 4H, H_{11}); 4.42 (t broad, 4H, H_{16}); 3.5–3.3 (m, 8H, H_{13}, $H_{13'}$); 1.98 (s, 12H, H_{19}); 1.8–1.5 (m, 12H, H_{14}, $H_{14'}$, H_{15}); 1.02 (t, J = 7.2 Hz, 6H, $H_{16'}$). ^{13}C NMR ($CDCl_3$) δ ppm: 171.9 (C_{17}); 156.3 (C_2); 149.9 (C_6); 148.6 (C_{12}); 146.9 (C_4); 137.1 (C_8); 129.4 (C_{10}); 124.2 (C_9); 121.2 (C_7); 120.5 (C_5); 118.6 (C_3); 112.1 (C_{11}); 66.0 (C_{16}); 56.8 (C_{18}); 51.3 and 50.9 (C_{13}, $C_{13'}$); 31.0 (C_{19}); 29.8 (C_{15}); 26.4 ($C_{14'}$); 24.1 (C_{14}); 20.7 ($C_{15'}$); 14.2 ($C_{16'}$). UV–visible (CH_2Cl_2): λ_{max} = 391 nm, ϵ_{max} = 40,200 l mol^{-1} cm^{-1}. Emission (CH_2Cl_2): λ_{em} = 495 nm. Anal.

Calc. (found) for $C_{50}H_{64}N_4O_4Br_2{\cdot}1.5CH_2Cl_2$: C, 57.69 (57.80); H, 6.30 (6.36); N, 5.22 (5.47).

*4.1.3. Dehydrohalogenation of **b***

In a Schlenk flask, bipyridine **b** (0.05 g; 0.059 mmol)

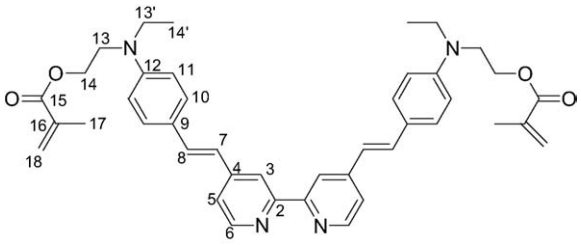

was dissolved in anhydrous DMF (5 ml). The mixture was then refluxed for 15 h. The solvent was then evaporated under vacuum. The product was washed first with pentane and finally with ether to afford **c** as a brown powder (0.032 g, 80%).

^{1}H NMR ($CDCl_3$) δ ppm: 8.7 (d broad, 4H, H_6, H_3); 7.6–7.4 (m, 8H, H_8, H_5, H_{10}); 7.02 (d, J = 16.6 Hz, 2H, H_7); 6.83 (d, J = 8.8 Hz, 4H, H_{11}); 6.14 (s large, 2H, H_{18}); 5.64 (s large, 2H, H_{18}); 3.65–3.60 (m, 4H, H_{13}); 3.55–3.45 (m, 4H, $H_{13'}$); 1.98 (s, 12H, H_{17}); 1.26 (t, J = 6.97 Hz, 6H, $H_{14'}$). MS (FAB) calc. for $C_{42}H_{49}N_4O_4Br_2$ $[M + H]^+$: 671, found: 671.

*4.1.4. [Fe(**b**)$_3$][PF$_6$]$_2$ (**1b**)*

In a mixture of acetone and water (20 ml/10 ml) were dissolved iron sulfate heptahydrate (0.063 g, 0.23 mmol) and the ligand **b** (0.38 g, 0.45 mmol). After sonication for 10 min, the mixture was stirred overnight at room temperature. The solution was then poured into an aqueous solution (50 ml) of KPF_6 (0.110 g, 0.6 mmol) leading to precipitation of the complex. The solid was then filtered off and washed with water (2 × 30 ml). The crude was dissolved in CH_2Cl_2, dried over $MgSO_4$, filtered and the solvent was removed under vacuum. After precipitation from dichloromethane/pentane, **1b** was recovered as a green powder (0.32 mg, 74%).

^{1}H NMR (CD_2Cl_2) δ ppm: 8.42 (s, 6H, H_3), 7.6–7.4 (m, 18H, H_{10}, H_8), 7.37 (d, J = 5.9 Hz, 6H, H_5), 7.25 (d, J = 5.9 Hz, 6H, H_6), 6.95 (d, J = 16.5 Hz, 6H, H_7), 6.76 (d, J = 8.8 Hz, 12H, H_{11}), 4.31 (t br, 12H, H_{14}), 3.65 (t br, 12H, H_{13}), 3.48 (q br, 12H, $H_{13'}$), 1.89 (s, 36H, H_{15}), 1.18 (t, J = 6.8 Hz, 36H, $H_{14'}$). ^{13}C NMR (CD_2Cl_2) δ ppm: 172.0 (C_{15}), 159.5 (C_2), 152.9 (C_6), 149.5 (C_{12}), 148.8 (C_4), 137.6 (C_8), 129.9 (C_{10}), 123.6 (C_5), 123.4 (C_9), 120.2 (C_3), 118.6 (C_7), 112.3 (C_{11}), 63.6 (C_{14}), 56.3 (C_{16}), 48.6 (C_{13}), 45.8 ($C_{13'}$), 30.9 (C_{17}), 12.4 ($C_{14'}$),. Anal. Calc. (found) for $C_{126}H_{144}N_{12}O_{12}Br_6P_2F_{12}Fe{\cdot}CH_2Cl_2$: C, 52.08 (51.62), H, 5.02 (5.02), N, 5.74 (5.82). UV–visible (CH_2Cl_2): λ_{max} = 456 nm (ILCT); ϵ = 138,000 l mol^{-1} cm^{-1}; λ = 589 nm (MLCT); ϵ = 56,000 l mol^{-1} cm^{-1}. Emission (CH_2Cl_2): λ_{em} = 621 nm. FTIR (KBr): $\nu_{(C=O)}$ = 1734 cm^{-1}, $\nu_{(PF6)}$ = 843 cm^{-1}.

*4.1.5. [Ru(**b**)$_3$][PF$_6$]$_2$ (**2b**)*

To a THF solution (15 ml) of **2a** (0.515 g, 0.25 mmol) was added triethylamine (0.25 ml; 1.6 mmol) and 2-bromoisobutyrylbromide (0.3 ml, 2.2 mmol). After one night stirring at room temperature, the solvent was removed under vacuum. The reaction mixture was dissolved in dichloromethane (100 ml) and washed with a saturated aqueous solution of $NaHCO_3$ (3 × 50 ml). The organic layer was dried over $MgSO_4$, filtered and the solvent was removed under vacuum. After precipitation from dichloromethane/pentane, **2b** was obtained as adark red powder (0.50 g, 70%).

^{1}H NMR (CD_2Cl_2) δ ppm: 8.42 (s, 6H, H_3); 7.6–7.4 (m, 24H, H_6, H_8, H_{10}); 7.32 (d, J = 5.6 Hz, 6H, H_5); 6.94 (d, J = 16.0 Hz, 6H, H_7); 6.70 (d, J = 8.5 Hz, 12H, H_{11}); 4.31 (t broad, 12H, H_{14}); 3.65 (t broad, 12H, H_{13}); 3.48 (q broad, 12H, $H_{13'}$); 1.82 (s, 36H, H_{17}); 1.13 (t, J = 7.2 Hz, 18H, $H_{14'}$). ^{13}C NMR (CD_2Cl_2) δ ppm: 172.0 (C_{15}); 159.5 (C_2); 152.9 (C_6); 149.5 (C_{12}); 148.8 (C_4); 137.6 (C_8); 129.9 (C_{10}); 123.6 (C_5); 123.4 (C_9); 120.2 (C_3); 118.6 (C_7); 112.3 (C_{11}); 63.6 (C_{14}); 56.3 (C_{16}); 48.6 (C_{13}); 45.8 ($C_{13'}$); 30.9 (C_{17}); 12.4 ($C_{14'}$). UV–visible (CH_2Cl_2): λ_{max} = 446 nm (ILCT); ϵ_{max} = 103,000 l mol^{-1} cm^{-1}; λ = 501 nm (MLCT); ϵ_{max} = 95,000 l mol^{-1} cm^{-1}. Emission (CH_2Cl_2): λ_{em} = 713 nm. IR (KBr): 1734 cm^{-1} ($\nu_{C=O}$); 843 cm^{-1} (PF_6).

*4.1.6. [Zn(**b**)$_3$][PF$_6$]$_2$ (**3b**)*

To a THF solution (10 ml) of **3a** (0.35 g, 0.17 mmol) was added pyridine (0.1 ml; 1.3 mmol) and a THF solution (5 ml) of 2-bromoisobutyrylbromide (0.17 ml, 1.4 mmol). After one night stirring at room temperature, the product was precipitated by addition of water (100 ml), filtered off, and washed with water (2 × 30 ml) and pentane (2 × 30 ml). The crude product was dis-

solved in CH_2Cl_2, dried over $MgSO_4$, filtered and the solvent was removed under vacuum. After precipitation from dichloromethane/pentane, **3b** was recovered as an orange powder (0.29 g, 60%).

^{1}H NMR (CD_2Cl_2) δ ppm: 8.43 (s, 6H, H_3), 7.78 (d, J = 5.5 Hz, 6H, H_6), 7.6–7.3 (m, 24H, H_8, H_5, H_{10}), 7.01 (d, J = 16 Hz, 6H, H_7), 6.79 (d, J = 8.6 Hz, 12H, H_{11}), 4.33 (t br, 12H, H_{14}), 3.67 (t br, 12H, H_{13}), 3.49 (q br, 12H, $H_{13'}$), 1.89 (s, 36H, H_{15}), 1.22 (t, J = 6.8 Hz, 18H, $H_{14'}$). ^{13}C NMR (CD_2Cl_2) δ ppm: 172.0 (C_{15}), 151.6 (C_2), 150.1 and 149.9 (C_{12} or C_2), 149.5 (C_4), 138.2 (C_8), 129.9 (C_{10}), 123.5 (C_5), 122.9 (C_9), 119.7 (C_3), 118.8 (C_7), 112.3 (C_{11}), 63.6 (C_{14}), 56.3 (C_{16}), 48.6 (C_{13}), 45.8 ($C_{13'}$), 30.9 (C_{17}), 12.4 ($C_{14'}$). Anal. Calc. (found) for $C_{126}H_{144}N_{12}O_{12}Br_6P_2F_{12}Zn$: C, 53.04 (53.64); H, 5.09 (5.15); N, 5.89 (6.25). UV–visible (CH_2Cl_2): λ_{max} = 448 nm; ϵ = 146,000 l mol^{-1} cm^{-1}. Emission (CH_2Cl_2): λ_{em} = 620 nm. FTIR (KBr): $\nu_{(C=O)}$ = 1734 cm^{-1}; $\nu_{(PF6)}$ = 843 cm^{-1}.

4.2. General procedure for the polymerization

Methyl methacrylate was polymerized using **1b**, **2b** and **3b** (50 mg, 1.7 × 10^{-2} mmol) as initiator (MMA/CuBr/*n*-propyl-2-pyridylmethanimine/initiator = 260:1:2:1). In a Schlenk tube, the initiator, MMA and CuBr(I) were dissolved into 2 ml of 1,2-dichlorobenzene and the solution was deoxygenated by three freeze-pump-thaw cycles. *N*-Propyl-2-pyridylmethanimine was added under argon and the solution was immediately immerged in an oil bath maintained at 90 °C. Samples were taken periodically using degassed syringes for conversion and molecular weight analysis. The copper was removed from the samples by passing through a column of neutral alumina plug (eluent: CH_2Cl_2), further precipitation in dichloromethane/pentane afforded the pure polymer.

Acknowledgements

The authors would like to thank the French *Ministère de la Recherche* (FNS-Programme nanostructures), the CNRS and the *Région Bretagne* (PRIR A2CA16) for financial support. We are grateful to J. Le Lannic (CMEBA) for running SEM experiments.

References

[1] (a) J.S. Wang, K. Matyjaszewski, J. Am. Chem. Soc. 117 (1995) 5614; (b) K. Matyjaszewski, J. Xia, Chem. Rev. 101 (2001) 2921.

[2] (a) M. Kato, M. Kamigaito, M. Sawamoto, T. Higashimura, Macromolecules 28 (1995) 1721; (b) T. Ando, M. Kato, M. Kamigaito, M. Sawamoto, Macromolecules 29 (1996) 1070.

[3] See for example: (a) C.J. Hawker, J.L. Hedrick, E.E. Malmström, M. Trollsas, M. Mecerreyes, G. Moineau, P. Dubois, R. Jérôme, Macromolecules 31 (1998) 213; (b) R.B. Grubbs, C.J. Hawker, J. Dao, J.M.J. Frechet, Angew. Chem. Int. Ed. Engl. 37 (1997) 2270; (c) X.S. Wang, N. Luo, S.K. Ying, Polymer 40 (1999) 4515; (d) X.S. Wang, N. Luo, S.K. Ying, Polymer 40 (1999) 4515; (e) Y. Nakagawa, P.J. Miller, K. Matyjaszewski, Polymer 39 (1998) 5163; (f) A. Heise, J.L. Hedrick, M. Trollsas, R.D. Miller, C.W. Frank, Macromolecules 32 (1999) 231; (g) S. Angot, K.S. Murthy, D. Taton, Y. Gnanou, Macromolecules 31 (1998) 7218.

[4] (a) J.E. Collins, C.L. Fraser, Macromolecules 31 (1998) 6715; (b) X. Wu, C.L. Fraser, Macromolecules 33 (2000) 4053; (c) R.M. Johnson, P.S. Corbin, C. Ng, C.L. Fraser, Macromolecules 33 (2000) 7404; (d) X. Wu, J.E. Collins, J.E. Mc Alvin, R.W. Cutts, C.L. Fraser, Macromolecules 34 (2001) 2812; (e) K. Peter, M. Thelakkat, Macromolecules 36 (2003) 1779.

[5] For recent reviews see: (a) U.S. Schubert, M. Heller, Chem. Eur. J. 7 (2001) 5253; (b) U.S. Schubert, C. Eschbaumer, Angew. Chem. Int. Ed. Engl. 41 (2002) 2892.

[6] T. Renouard, H. Le Bozec, Eur. J. Inorg. Chem. (2000) 229.

[7] (a) O. Maury, J.P. Guégan, T. Renouard, A. Hilton, P. Dupau, N. Sandon, L. Toupet, H. Le Bozec, New J. Chem. 25 (2001) 1553; (b) T. Renouard, H. Le Bozec, I. Ledoux, J. Zyss, Chem. Commun. (1999) 871; (c) K. Sénéchal, O. Maury, H. Le Bozec, I. Ledoux, J. Zyss, J. Am. Chem. Soc. 124 (2002) 4561.

[8] S. Brasselet, S. Bidault, J. Zyss, C. R. Phys. 3 (2002) 479.

[9] Preliminary communication: L. Viau, M. Even, O. Maury, D. Haddleton, H. Le Bozec, Macromol. Rapid Commun. 24 (2003) 630.

[10] T. Le Bouder, L. Viau, J.P. Guégan, O. Maury, H. Le Bozec, Eur. J. Org. Chem. (2002) 3024.

[11] T. Le Bouder, O. Maury, H. Le Bozec, A. Bondon, K. Costuas, E. Amouyal, J. Zyss, I. Ledoux, J. Am. Chem. Soc. 125 (2003) 12884.

[12] (a) D.M. Haddleton, C.B. Jasieczek, M.J. Hannon, A.J. Shooter, Macromolecules 30 (1997) 2190; (b) D.M. Haddleton, M.C. Crossman, B.H. Dana, D.J. Duncalf, A.M. Heming, D. Kukulj, A.J. Shooter, Macromolecules 32 (1999) 2110.

[13] (a) G. Moineau, M. Minet, P. Dubois, P. Teyssié, T. Senninger, R. Jérôme, Macromolecules 32 (1999) 27; (b) K. Matyjaszewski, S. Coca, S.G. Gaynor, M. Wei, B.E. Woodworth, Macromolecules 31 (1998) 5967.

[14] L. Viau, S. Bidault, O. Maury, S. Brasselet, I. Ledoux, J. Zyss, E. Ishow, K. Nakatani, H. Le Borec, J. Am. Chem. Soc. 126 (2004) 8386.

[15] R.N. Keller, H.D. Wycoff, Inorg. Synth. 2 (1947) 1.